

# ADAPTIVE INDUCTOR FOR VIBRATION DAMPING IN PRESENCE OF UNCERTAINTY

**B. Mokrani<sup>\*</sup>, I. Burda<sup>†</sup>, Z. Tian<sup>\*</sup>, A. Preumont<sup>\*</sup>**

<sup>\*</sup>Active Structures Laboratory, Université Libre de Bruxelles

50, Av. F. D. Roosevelt, 1050 Brussels, Belgium

bilal.mokrani@ulb.ac.be, zhui.tian@ulb.ac.be, andre.preumont@ulb.ac.be

<sup>†</sup> Babes Bolyai University

1, Mihail Kogalniceanu Street, Cluj-Napoca 400084, Romania

ioan\_burda@yahoo.com

**Keywords:** Smart structures, piezoelectric shunt, RL shunt, adaptive shunt, damping.

**Summary:** *This paper considers the RL shunt damping of vibration with a piezoelectric transducer, of a structure with a variable natural frequency. The inductive shunt damping is notorious for not being robust when the natural frequency of the electrical circuit does not match the natural frequency of the structure. In the proposed implementation, the shunted piezoelectric transducer is supplemented with a small additional one (with open electrodes) measuring the mechanical extension of the structure at the location of the transducer. The adaption strategy uses the property that, at resonance, the electric charge in the shunted transducer is in quadrature of phase with the mechanical strain at the location of the transducer (i.e. the voltage in the transducer with open electrodes). A Phase Shift to Voltage Converter, inspired from the Phase Locked Loop technique (PLL), is built to evaluate the phase shift between these two signals and to adapt the (synthetic) inductor  $L$  via a voltage controlled resistor, involving a photoresistor. The proposed strategy is supported by simulations and experimental results. .*

## 1. INTRODUCTION

Several piezoelectric shunt damping techniques for structural damping have been proposed during the last two decades. Typically, a piezoelectric transducer is attached to the structure to convert the vibratory energy into electrical energy and an electrical circuit is connected to its electrodes to dissipate the transformed energy.

The simplest piezoelectric shunt involves a single resistor  $R$  tuned properly to damp a single vibration mode, it is robust but inefficient. The linear RL shunt provides better performances; it involves a resistor and an inductor and it works as a dynamic absorber [5][6]: The piezoelectric transducer, being an electrical capacitance, when it is connected to the inductor, the resulting circuit is resonant. If the electrical frequency is tuned on the natural frequency of the structure, then the mechanical vibration excites the electrical resonance; the resistor is used to dissipate

the transformed energy and it can be mounted in series or in parallel with the inductor [7]. Damping several modes is also possible [8], by involving several RL branches.

Inductive shunt is notorious for requiring huge inductors and being very sensitive to the variation of the electrical frequency with respect to the natural frequency of the targeted mode. These problems are addressed by the Synchronized Switch Damping on Inductor shunt, referred to as SSDI [10]. It is a nonlinear shunt involving a synchronized switch and a very small inductor, and it offers similar performance as the RL shunt [14]. However, it requires complex implementation and it is very sensitive to the switching synchronization. Other non-linear shunts, based on the same concept as the SSDI, involving synchronized switches and voltage sources exist too [12].

Another way to overcome the problems related to the RL shunt is to use active synthetic inductors, called *gyrators* [4], and to adapt the value of the inductor when the resonance frequency of the targeted mode changes (in such a way that the electrical frequency matches the resonance frequency of the targeted mode). The adaptation can be based on two approaches: (i) the first approach consists of choosing the inductor which minimizes the RMS value of the vibration level [9] (e.g. voltage across the electrodes of the piezoelectric transducer); (ii) the second approach consists of tuning the inductor based on the fact that at resonance, the electrical charge  $Q$  flowing in the circuit and the strain at the location of the piezoelectric transducer are in quadrature of phase, only if the electrical frequency matches the natural frequency of the structure[2]. In this paper we consider an adaptive RL shunt based on the second approach.

The use of the relative phase shift between the electrical charge and the strain (or velocity), for the adaptation of the inductor, has been first proposed in [2] [3]. The relative phase shift between the reference signals is estimated based on the mean value of their product: when the signals are in phase the product is always positive and inversely when they are in antiphase, it is zero only when the signals are in quadrature of phase. The measurement system is performed using analog circuits and the output is then used to control a voltage controlled resistor based on a field-effect transistor (FET).

In this paper we propose an adaptive RL shunt damping using a voltage controlled synthetic inductor, based on a voltage controlled photoresistive opto-isolator, referred to as *vactrol*. A new phase shift to voltage converter circuit has been built to control the adaptive inductors. The circuit, inspired from Phase Locked Loop technique (PLL), utilises a phase detector to measure in real time the relative phase between the voltage drop in the inductor and the voltage of a small additional piezoelectric transducer. The output signal is then used by a DSP to control the inductor.

The paper is organized in three main parts. The first part discusses the principle of the linear RL shunt and the effect of parameters detuning on simple single degree of freedom system.

The second part discusses the adaptive shunt and the importance of the relative phase between the strain and the electrical charge in the circuit. Finally, the third part is devoted to the experimental implementation of the adaptive RL shunt on a cantilever beam and to the description of the various circuits.

## 2. LINEAR RL SHUNT

Consider the one-dimensional spring-mass system of Fig.1 subjected to an external disturbance  $d$  and equipped with a linear piezoelectric stack working according to the  $d_{33}$  mode. The

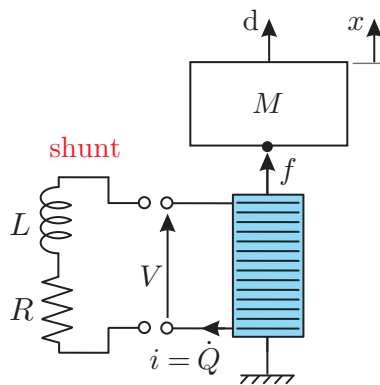


Figure 1. One-dimensional spring-mass system equipped with a piezoelectric linear transducer (the inherent damping of the system is neglected for the sake of simplicity).

constitutive equations of the piezoelectric transducer<sup>1</sup> are:

$$\begin{Bmatrix} V \\ f \end{Bmatrix} = \frac{K_a}{C(1-k^2)} \begin{bmatrix} 1/K_a & -nd_{33} \\ -nd_{33} & C \end{bmatrix} \begin{Bmatrix} Q \\ x \end{Bmatrix} \quad (1)$$

where  $V$  is the electrical voltage between its electrodes,  $Q$  the electrical charge stored,  $x$  its elongation and  $f$  the force applied at its tips;  $K_a$  is the stiffness of the transducer in short-circuit (i.e.  $V = 0$ ),  $C$  is the electrical capacitance when no forces are applied (i.e.  $f = 0$ ),  $d_{33}$  is the piezoelectric constant, and  $k$  is the electro-mechanical coupling coefficient, it measures the capability of the transducer of converting mechanical energy into electrical energy and vice versa.

The mass  $M$  is governed by:

$$M\ddot{x} = -f + d \quad (2)$$

<sup>1</sup>In practice, the transducer is mounted with a prestressing structure to prevent the splitting of the PZT slices under traction. This can be represented by a linear spring  $K_1$  mounted in parallel to the piezoelectric stack. By considering the prestressing spring  $K_1$ , one can find readily the same form of the piezoelectric constitutive equations with the effective properties:  $K_a^* = K_a + K_1$ ,  $C^* = C(1 - k^2 + \nu k^2)$ ,  $d_{33}^* = \nu d_{33}$  and  $k^{*2} = k^2 \nu / (1 - k^2 + \nu k^2)$ , where  $\nu$  is the fraction of strain energy in the transducer defined as:  $\nu = K_a / (K_1 + K_a)$ , see [11].

After substituting the constitutive equations of the transducer, one obtains the governing equations of the whole electromechanical system of Fig.1 as:

$$M\ddot{x} + \frac{Ka}{(1-k^2)}x = d + \frac{nd_{33}K_a}{C(1-k^2)}Q \quad (3)$$

$$V = \frac{1}{C(1-k^2)}Q - \frac{nd_{33}K_a}{C(1-k^2)}x \quad (4)$$

by introducing the definition of the resonance frequency (with open-electrodes):

$$\Omega_n = \sqrt{\frac{K_a}{(1-k^2)M}},$$

and using the Laplace transform, one gets

$$x = \frac{1}{M} \frac{1}{(s^2 + \Omega_n^2)}d + \frac{nd_{33}}{C} \frac{\Omega_n^2}{(s^2 + \Omega_n^2)}Q \quad (5)$$

when the piezoelectric transducer is shunted, in series, on a linear RL circuit, the voltage  $V$  and the charge  $Q$  are related through the impedance of the shunt:

$$V = -L\ddot{Q} - R\dot{Q} \quad (6)$$

leading to:

$$Q + RC(1-k^2)\dot{Q} + LC(1-k^2)\ddot{Q} = nd_{33}K_ax \quad (7)$$

and, using the definitions of electrical frequency and damping, such that:

$$\omega_e = \frac{1}{\sqrt{LC(1-k^2)}}, \text{ and } 2\xi_e\omega_e = \frac{R}{L}$$

one gets (after using the Laplace transform):

$$Q = \frac{nd_{33}K_a\omega_e^2}{(s^2 + 2\xi_e\omega_e s + \omega_e^2)}x \quad (8)$$

Eq.(5) and Eq.(8) describes the full dynamics of the system.

## 2.1 Optimal tuning

The transmissibility between the mass displacement  $x$  and the disturbance force  $d$  is obtained by substituting<sup>2</sup> Eq.(8) into Eq.(5):

$$\frac{x(s)}{d(s)} = \frac{1}{M} \frac{s^2 + 2\xi_e\omega_e s + \omega_e^2}{s^4 + 2\xi_e\omega_e s^3 + (\omega_e^2 + \Omega_n^2)s^2 + 2\xi_e\omega_e\Omega_n^2 s + \omega_e^2\Omega_n^2} \quad (9)$$

---

<sup>2</sup>The definition of  $k^2$  has been used, where  $k^2 = \frac{n^2 d_{33}^2 K_a}{C}$ .

where

$$\omega_n = \sqrt{\frac{K_a}{M}}$$

is the resonance frequency of the system with short-circuited electrodes.

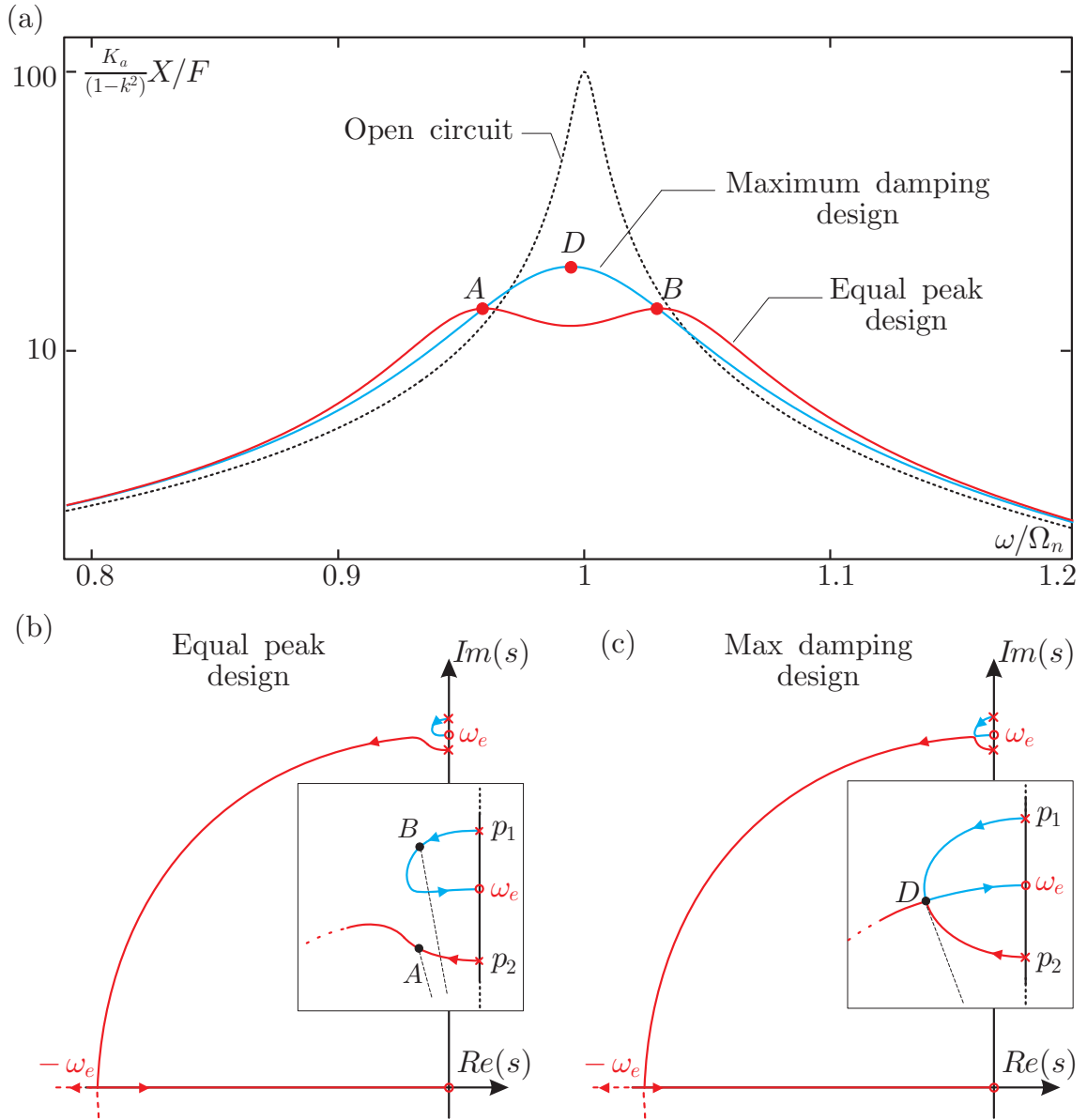


Figure 2. *RL* shunt tuning: (a) frequency response of the mass  $x/d$  with open circuited electrodes, with *RL* shunt tuned according to the equal peak design and with *RL* shunt tuned according to the maximum damping design; (b) and (c) the root locus of the system when the resistor  $R$  varies from  $\infty$  (open circuit) to 0 (short circuit), with the electrical frequency tuned, respectively, according to the equal peak design and to the maximum damping design.

Equation (9) can be used as a metric for the tuning of the RL circuit components. Depending on the frequency content of the excitation, the RL circuit can be tuned in two ways [7](other types of design are also possible):

- **Equal peak design**, where the circuit is tuned to minimize the  $H_\infty$  norm of the mass response  $x$ , i.e. to minimize the maximum of the frequency response  $x(\omega)/d(\omega)$ . This design is usually referred to as the equal peak design because it results in a double peak with equal amplitudes of the frequency response, Fig.2. The optimal parameters are obtained by tuning the electrical frequency  $\omega_e$  as:

$$\frac{\omega_e^*}{\omega_n} = \frac{1}{\sqrt{1-k^2}}, \quad \text{or} \quad \frac{\omega_e^*}{\Omega_n} = 1, \quad (10)$$

and the electrical damping  $\xi_e$  as

$$\xi_e^* = \sqrt{\frac{3}{8}}k \quad (11)$$

- **Maximum damping (stability) design**: In this design, the RL circuit is tuned to maximizes the damping of the targeted mode, and thus, the stability of the system, Fig.2.c. The optimal tuning of the RL circuit is achieved when the targeted mode and the electrical mode have the same frequency and damping; it is achieved by tuning the electrical frequency  $\omega_e$  as

$$\frac{\omega_e^* \omega_n}{\Omega_n^2} = 1, \quad \text{or} \quad \frac{\omega_e^*}{\omega_n} = \frac{1}{1-k^2} \quad (12)$$

and the electrical damping as

$$\xi_e^* = k \quad (13)$$

Next, we will consider only the equal peak design and analyse the effect of the electrical frequency and damping variation on the performance.

Finally, one should notice that for a multi degree of freedom system, the generalized electromechanical coupling factor  $K_i$ , of a specific mode  $i$ , should be used instead of  $k^2$ . It is defined as:

$$K_i^2 = \frac{\Omega_i^2}{\omega_i^2} - 1,$$

where  $\Omega_i$  and  $\omega_i$  are, respectively, the resonance frequencies of mode  $i$  with open electrodes and short-circuited electrodes.

### 3. ROBUSTNESS OF RL SHUNT

The three main parameters that may vary and affect the tuning of the RL shunt are the inherent capacitance of the piezoelectric transducer  $C$ , the electromechanical coupling factor  $k$  and the resonance frequency  $\Omega_n$ ; a variation of one of the these parameters deviates the value of the electrical parameters from being optimal, and thus, affects the performance of the RL shunt. In this section, we study the effect of the electrical parameters detuning on the performance of the RL shunt.

### 3.1 Sensitivity to $R$

Figure 3 shows the influence of the deviation from the optimal tuning of the resistor  $R$ , on the attenuation generated in the response of the structure (the  $H_\infty$  norm of  $x/d$  is considered). An error of the tuning of  $\pm 30\%$  affects the performance by only  $10\%$ , independently from  $k$ . The figure shows that the RL shunt is weakly sensitive to mistuning of the resistor  $R$ .

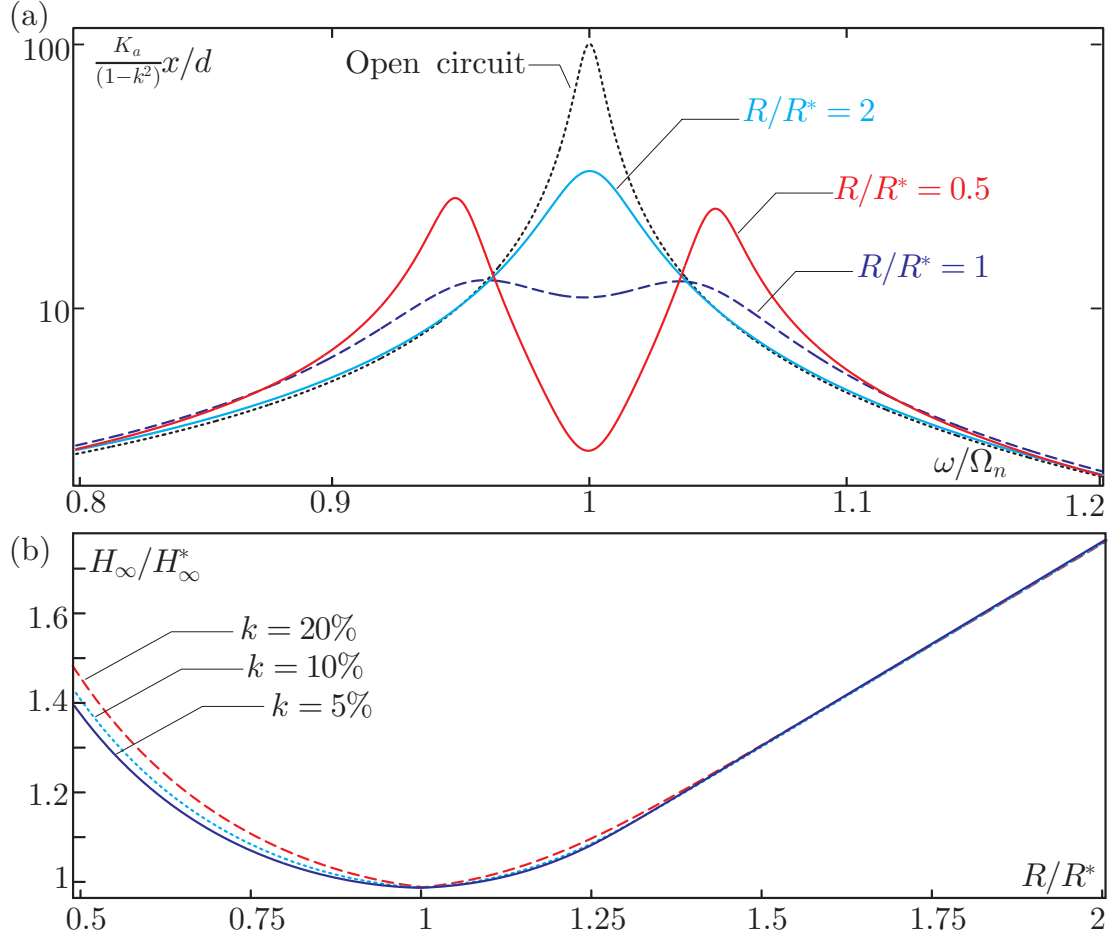


Figure 3. Influence of the resistor tuning  $R$  on the attenuation generated. The maximum attenuation (corresponding to  $H_\infty^*$ ) is obtained for  $\xi_e^* = \sqrt{3/8k}$ . (a) Frequency response  $x/d$  for various values of  $R$  ( $k = 10\%$ ); (b)  $H_\infty^*$  of  $H_\infty^*$  as a function of the variation of  $R$ .

### 3.2 Sensitivity to $\omega_e$

The performance of the RL shunt is very sensitive to the variability of the resonance frequency of the targeted mode with respect to the electrical frequency  $\omega_e$ , and thus to  $L$ ; this sensitivity is illustrated in Fig.4. The figure shows that an error on the electrical frequency of  $\pm 10\%$  reduces the attenuation by a factor 2 to 4, for  $k$  varying from 20% to 5%. This high sen-

sitivity justifies the need of an adaptive tuning of the inductor. The sensitivity to the electrical tuning  $\omega_e$  tends to decrease when the electromechanical coupling factor increases.

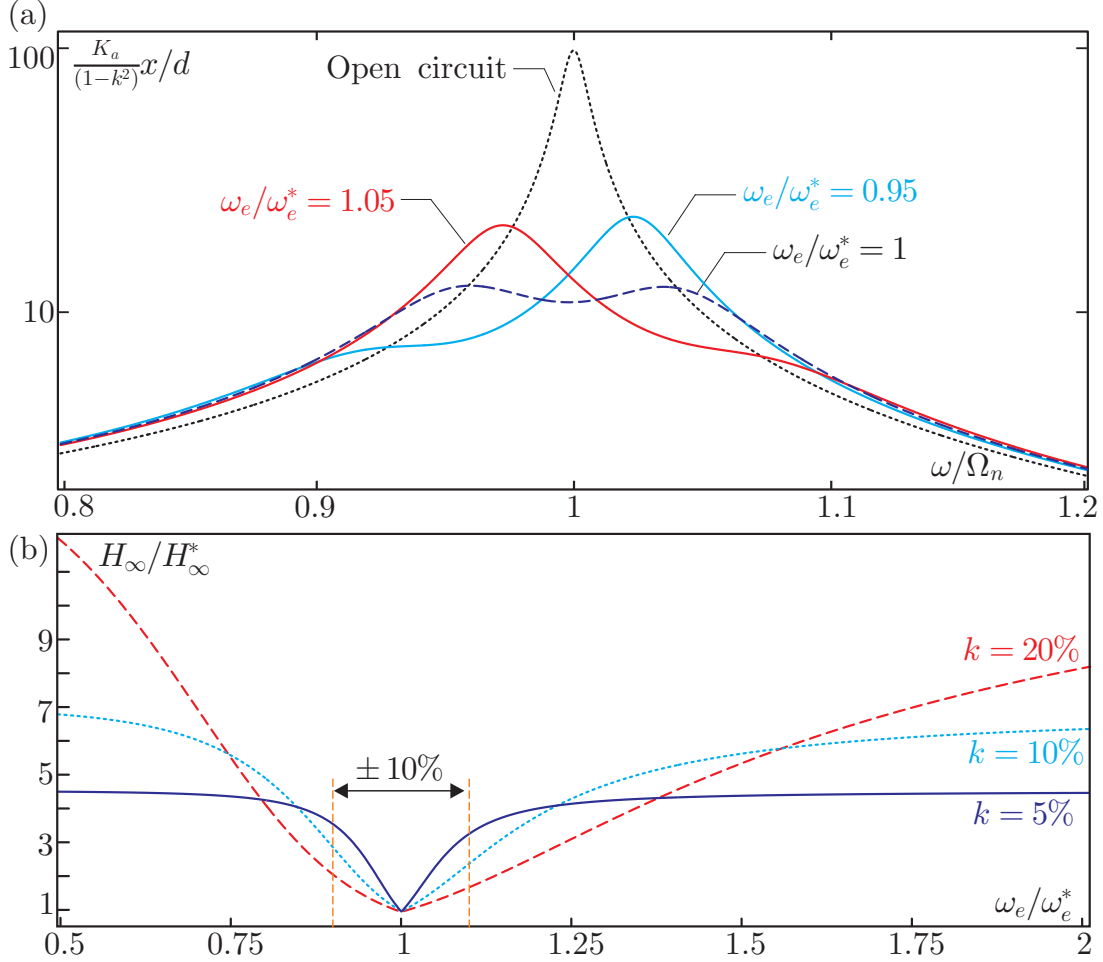


Figure 4. Influence of the electrical frequency tuning  $\omega_e$  on the attenuation generated. The maximum attenuation (corresponding to  $H_\infty^*$ ) is obtained for  $\omega_e^* = \Omega_n$ . (a) Frequency response  $x/d$  for various values of  $\omega_e$  ( $k = 10\%$ ); (b)  $H_\infty^*$  of  $H_\infty^*$  as a function of the variation of  $\omega_e$ .

#### 4. ADAPTIVE RL SHUNT

A simple way to recover the degradation of the performance of the RL shunt, due to uncertainties on the electrical frequency, is to adapt the value of  $L$  so as to preserve the optimal tuning. In this section, we show the effect of the electrical frequency detuning on the relative phase shift between the electrical charge  $Q$  and the displacement  $x$ . Then we consider an adaptive inductor  $L$ , based on the fact that, at resonance, the relative phase shift between  $Q$  and  $x$  is  $\pi/2$  only if  $\omega_e = \Omega_n$  [Eq.(10)].



#### 4.1 Adaptation law

Consider again the system of Fig.1 with the piezoelectric transducer shunted on a RL circuit. If the disturbance force  $d$  is a band-limited white noise, then, from Eq.(9), the response  $x$  is a narrow band random process of *central frequency* equal to  $\Omega_n$ ; it can be considered as a sine wave with slowly varying amplitude and frequency (around  $\Omega_n$ ). As a first approximation, it can be represented as:

$$x = A \sin \Omega_n t \quad (14)$$

Therefore, according to Eq.(8), since  $x$  is nearly harmonic, the electrical charge  $Q$  is also harmonic of the form:

$$Q = \alpha A \sin(\Omega_n t + \Delta\phi) \quad (15)$$

where  $\alpha$  is the magnitude of  $Q/x$  evaluated at  $s = j\Omega_n$ , and  $\Delta\phi$  is its phase given by:

$$\Delta\phi = \arg(Q/x) = \arg \left( nd_{33}K_a \frac{\omega_e^2}{-\Omega_n^2 + 2\xi_e\omega_e\Omega_n j + \omega_e^2} \right) \quad (16)$$

From Eq.(16), one gets for:

- $\Omega_n \gg \omega_e$ :  $\Delta\phi \simeq -\pi$ ,
- $\Omega_n \ll \omega_e$ :  $\Delta\phi \simeq 0$ ,
- $\Omega_n = \omega_e$ , which corresponds to the optimal tuning of the equal peak design [Eq.(10)]:

$$\Delta\phi = \arg \left( \frac{nd_{33}K_a}{2\xi_e j} \right) = -\frac{\pi}{2}$$

Therefore, by measuring the relative phase between  $x$  and  $Q$ , it is possible to detect the direction of the electrical frequency detuning and to compensate it by adapting the inductance  $L$  in such a way to keep  $\Delta\phi = -\pi/2$ .

The relative phase between  $x$  and  $Q$  must be  $\Delta\phi = -\pi/2$ , so that  $Q$  is in antiphase with the velocity  $\dot{x}$ , in order to produce a pure positive damping effect at resonance where most of vibration energy is concentrated. Indeed, the RL shunt has a damping effect only around the resonance, within the bandwidth where the relative phase, between  $x$  and  $Q$ ,  $-3\pi/4 < \Delta\phi < -\pi/4$ , and an amplification effect outside this bandwidth. This explains the high sensitivity of the RL shunt to frequency detuning when the electromechanical coupling factor  $k$  is small, which is translated by a small electrical damping  $\xi_e^*$  and thus a quick decrease of the relative phase around the resonance frequency.

## 4.2 Measurement of $Q$

In practice, it is not easy to measure  $Q$  explicitly. However, if one considers the measurement of the voltage of the inductor  $V_L$ :

$$V_L = -L\ddot{Q} = -Ls^2Q = L\omega^2Q,$$

then, one obtains a signal  $V_L$  always in phase with  $Q$ . The relationship between  $V_L$  and  $x$  is then obtained by multiplying Eq.(8) by  $-Ls^2$ :

$$\frac{V_L}{x} = nd_{33}K_a \frac{-L\omega_e^2 s^2}{s^2 + 2\xi_e\omega_e s + \omega_e^2} \quad (17)$$

From this equation, the relative phase between  $x$  and  $V_L$  is deduced as

$$\Delta\phi = \arg(V_L/x) = \arg\left(nd_{33}K_a \frac{L\omega_e^2\Omega_n^2}{-\Omega_n^2 + 2\xi_e\omega_e\Omega_n j + \omega_e^2}\right) \quad (18)$$

leading to the same relative phase as that of Eq.16. Once again, when  $\omega_e = \Omega_n$ :

$$\Delta\phi = \arg\left(\frac{nd_{33}K_a L\Omega_n^2}{2\xi_e j}\right) = -\frac{\pi}{2} \quad (19)$$

Finally, the maximum performance of the RL shunt can be guaranteed by tuning the electrical frequency in such a way to keep  $\Delta\phi = -\pi/2$ .

## 4.3 Sensitivity of $\Delta\phi$

Consider now the frequency response of  $V_L/x$  shown in Fig.5. The figure shows the effect of the electrical frequency detuning on the magnitude and the relative phase  $\Delta\phi$ . An optimal tuning of  $\omega_e$  corresponds to a phase shift of exactly  $-\pi/2$  at  $\omega = \Omega_n$ , and the peak of magnitude (which corresponds to the frequency at which the RL shunt is more efficient). For a deviation of  $\pm 5\%$  of  $\omega_e$ , the curves are right or left shifted along the frequency axis and the relative phase  $\Delta\phi$  at  $\omega = \Omega_n$  varies depending on the variation of the electrical frequency. This demonstrates the high sensitivity of  $\Delta\phi$  to the variation of  $\omega_e$  and also justifies the high sensitivity of the performance of the RL shunt to the detuning of  $\omega_e$ . For a very small electrical damping  $\xi_e$ , which corresponds to a smaller electromechanical coupling factor  $k$ , this sensitivity is much pronounced.

Figure 6 shows the effect of the resistor detuning  $R$  on the magnitude and the phase of  $V_L/x$ . For the various values of  $R$ , the relative phase  $\Delta\phi$  at  $\omega = \Omega_n$  is not sensitive to the resistor detuning. Once a gain, this justifies the low sensitivity of the RL shunt performance to the tuning of the resistor  $R$ .

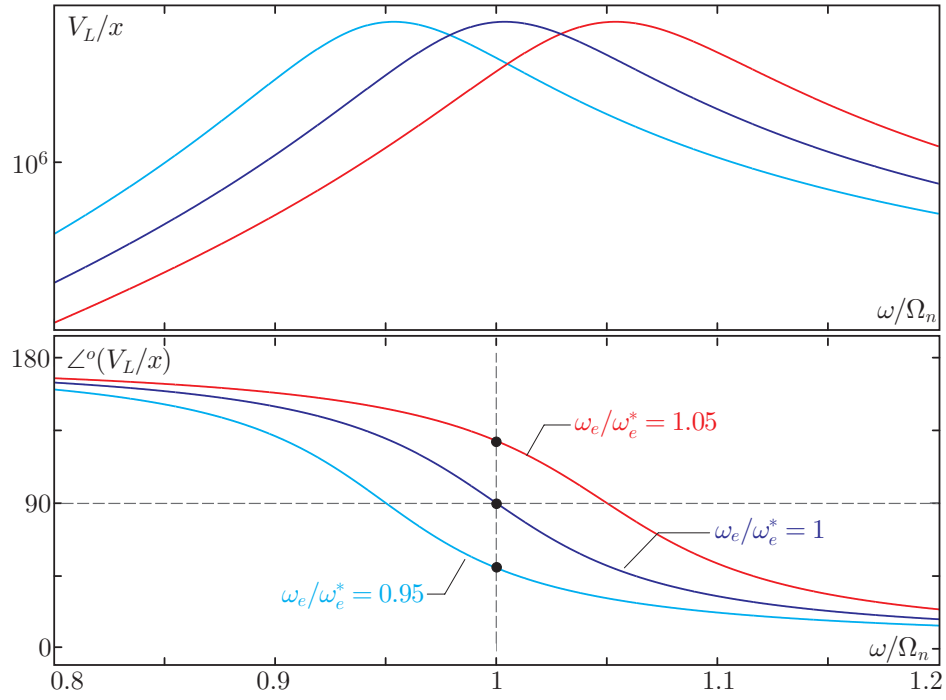


Figure 5. Magnitude and phase of  $V_L/x$ , for various tuning of the electrical frequency  $\omega_e$  ( $k = 10\%$ , corresponding to  $\xi_e = 6.1\%$ ).

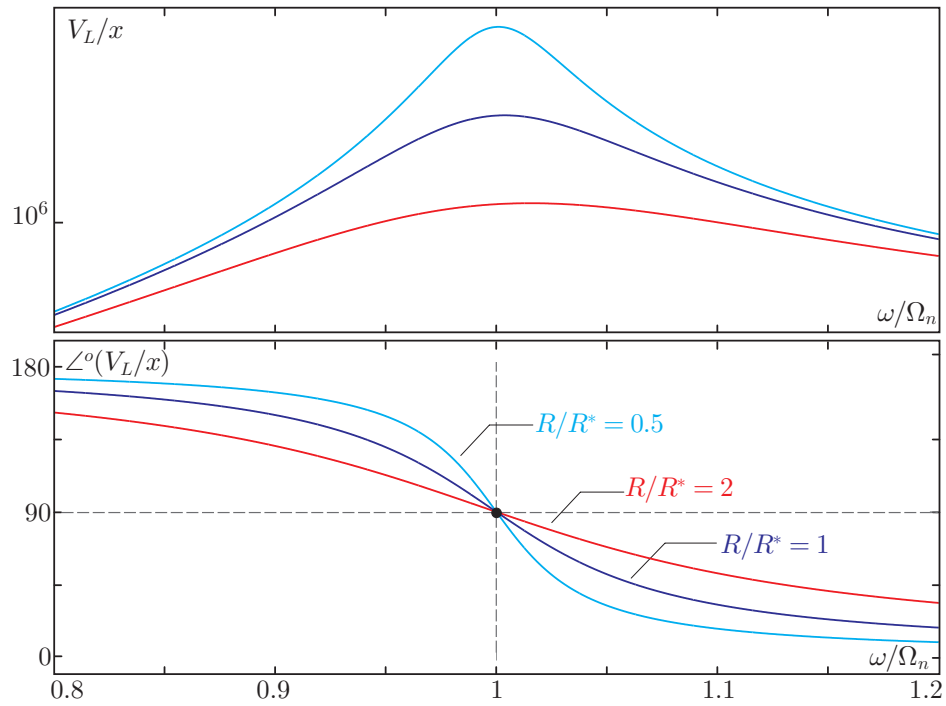


Figure 6. Magnitude and phase of  $V_L/x$ , for various tuning of the resistor  $R$  (or electrical damping  $\xi_e$ ).

## 5. EXPERIMENTS

### 5.1 Setup

The adaptive RL shunt has been implemented experimentally on a cantilever beam. The experimental setup is schematized in Fig.7. The structure consists of a lightly damped cantilever aluminum beam on which 2 PZT patches are glued close to the clamp, with opposite polarization and in front of each other. An optional mass is added at the tip of the beam using small strong magnets to allow the modification of the resonance frequency during operation. The excitation consists of a force applied by a voice-coil at the beam tip with a collocated measurement of the velocity using a non-contact laser vibrometer. The excitation is a band-limited white noise in the frequency range  $[80 - 180]Hz$ , to ensure the excitation of the first flexural mode only.

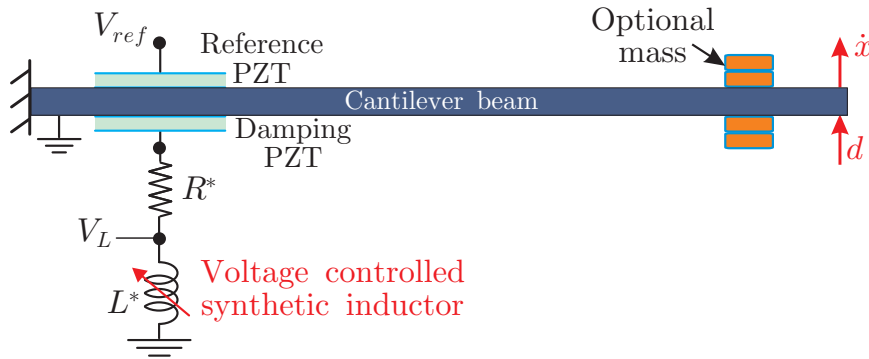


Figure 7. Experimental setup: Cantilever aluminium beam equipped with two PZT patches attached with a conductive glue. The beam, being conductive, is used as a common electrical ground.

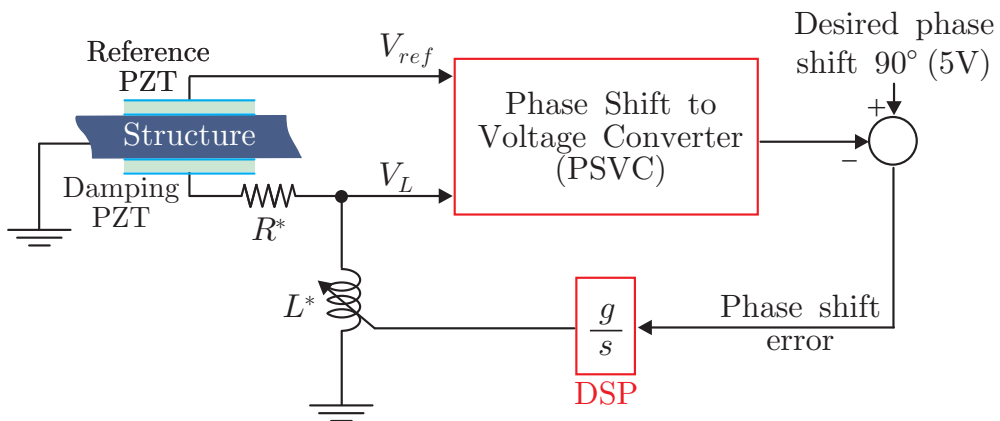


Figure 8. Principle of the the adaptive inductance control.

The implemented adaptive RL shunt is schematized in Fig.8. One PZT patch is used for the damping and it is shunted in series on a tunable resistor  $R$  and a voltage controlled synthetic

inductor  $L$ . The second PZT is used as a reference, since its voltage  $V_{ref}$  is proportional to the strain at its location, and thus, with analogy to the single degree of freedom system, it represents the measurement of  $x$ . The relative phase between  $V_L$  and  $V_{ref}$  is measured using a dedicated circuit, and compared to the desired relative phase shift ( $-\pi/2$  for an equal peak design). Then, the relative phase error is integrated using a dSpace DSP and the output is used as a command of the voltage controlled synthetic inductor.

## 5.2 Electrical circuits

The voltage controlled synthetic inductor is implemented based on the schematic shown in Fig.9, referred to as Antoniou's circuit. The value of the inductor can be tuned by simply tuning the resistor  $R_4$ , using a resistive optoisolator, called vactrol. Fig.10 shows the control circuit of the resistor  $R_4$ , involving a vactrol; by varying the voltage source from 0 to 10 Volts, the value of the resistor varies from  $100k\Omega$  to  $2k\Omega$ . One should notice that the relationship between  $R_4$  and the command voltage is not linear, but this non-linearity has no big effect on the tuning since the system is controlled in closed loop.

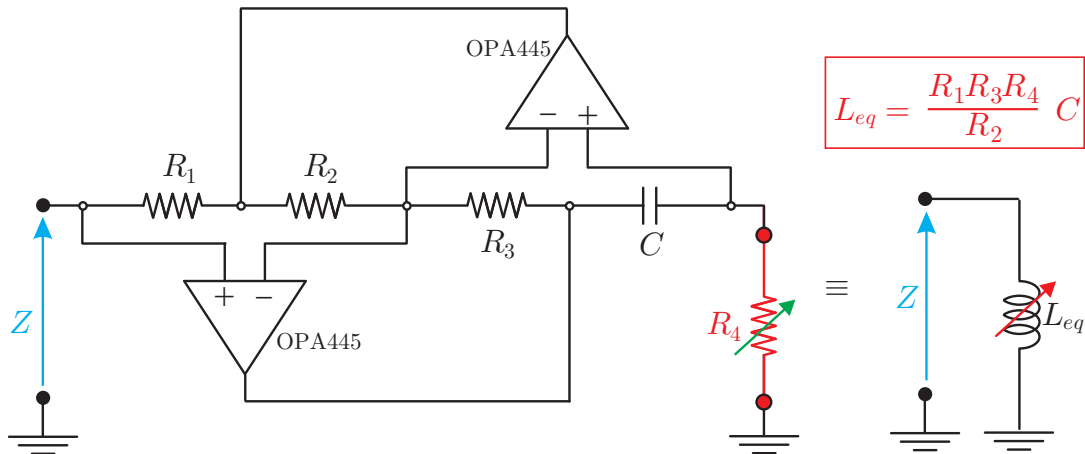


Figure 9. Voltage controlled synthetic inductor based on Antoniou circuit.

The Phase Shift to Voltage Converter circuit has been built using two different blocs, as shown in Fig.11. The first block is used to convert the harmonic signals to two square signals. Then, these square signals are used by the phase detector of a Phase Locked Loop circuit (from 74hc/hct4046A integrated PLL circuit). The output of the phase detector circuit is a voltage proportional to the relative phase between the two signals  $V_L$  and  $V_{ref}$ : the relationship between the output of the circuit and the relative phase is linear and varies from 0 to 10 volt for a phase shift varying from  $0^\circ$  to  $180^\circ$ . However, the circuit involves a low-pass filter of bandwidth of around 10Hz, which should be considered for the design of the controller.

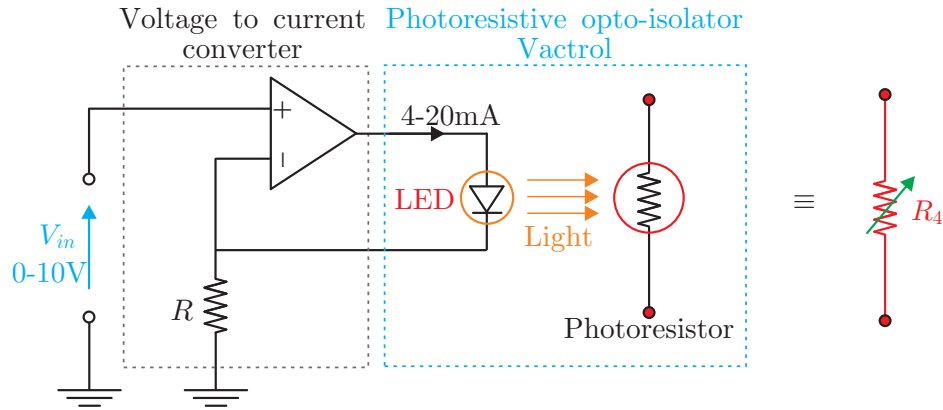


Figure 10. Voltage controlled resistor  $R_4$ , involving a resistive opto-isolator, Vactrol.

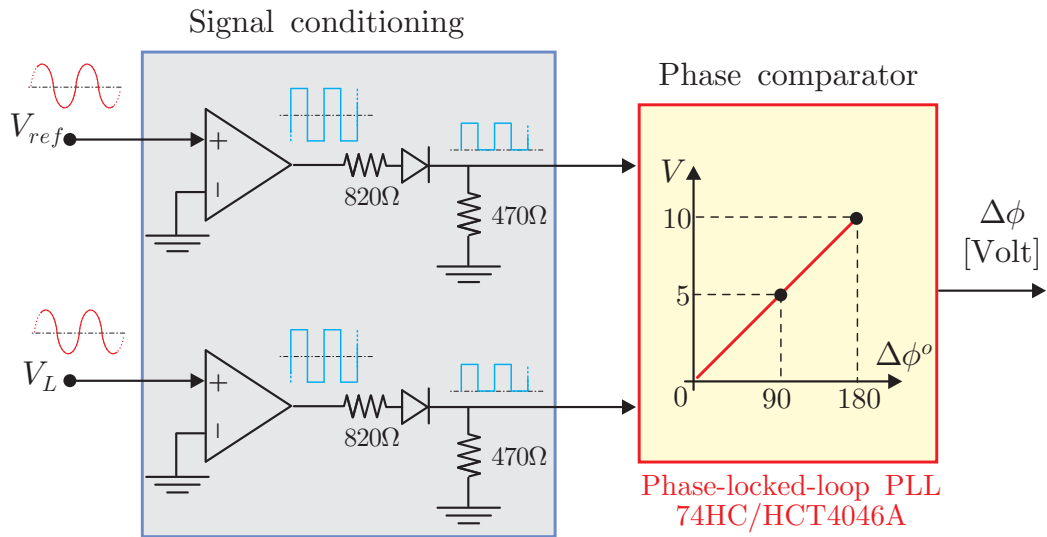


Figure 11. Phase Shift to Voltage Converter circuit based on a Phase Locked Loop circuit (PLL).

### 5.3 Results

Figure 15 shows the frequency response of the beam to a band limited white noise in the frequency range [80 to 180] Hz (including only the first flexural mode). The figure shows the effect of the electrical frequency tuning  $\omega_e$  on the RL shunt performance. Fig.13 shows the magnitude and phase of  $V_L/V_{ref}$  for the various tuning of  $\omega_e$ . In agreement with the simulations, when  $\omega_e = \Omega_n$ , the relative phase  $\Delta\phi$  is exactly<sup>3</sup>  $+\pi/2$  at  $\omega = \Omega_n$ . When the electrical frequency is mistuned, the relative phase becomes smaller or greater than  $\pi/2$ , depending whether  $\omega_e > \Omega_n$  or  $\omega_e < \Omega_n$ .

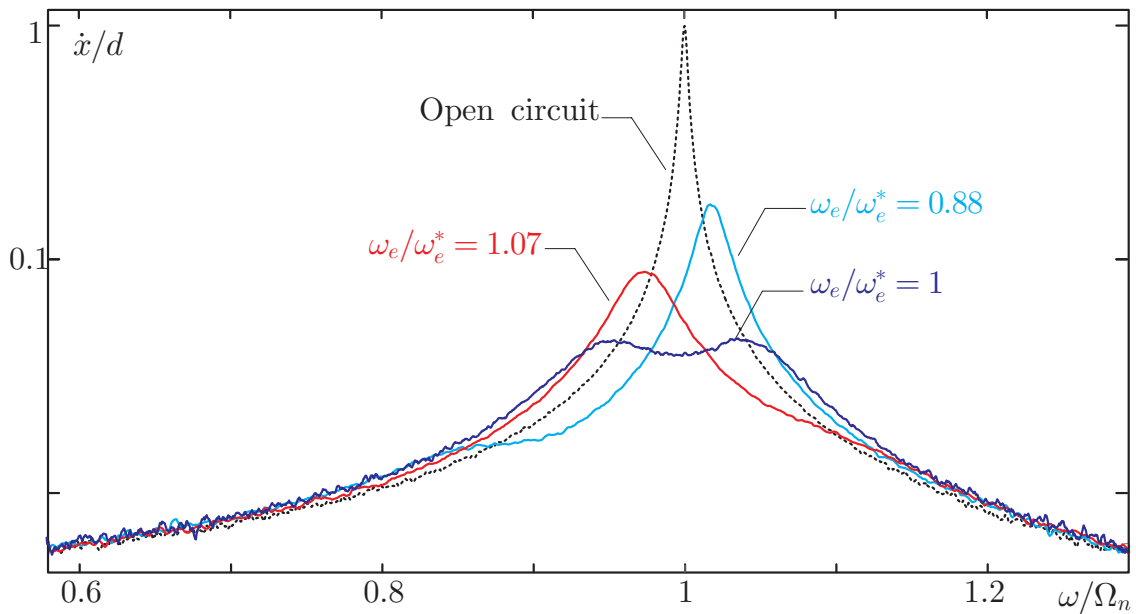


Figure 12. Frequency response of the beam for various values of  $\omega_e$ .

Figure 14 shows the time response of  $V_L$  and  $V_{ref}$  for the various tuning of the electrical frequency  $\omega_e$ . When the vibration level is high (i.e. the instantaneous frequency is  $\Omega_n$ ), the relative phase shift between the signals is in a good agreement with the predictions, for the various values of  $\omega_e$ .

#### Adaptive RL shunt

Figure 15 shows the response of the structure when the adaptive RL shunt is implemented according to the schematic of Fig.8. The value of  $L$  is tuned automatically in real time, via the feedback loop, and the feedback controller is a simple integrator. Since the adaptive inductor and the Phase Shift to Voltage Converter have a slow dynamics (of about 10Hz), the bandwidth of the controller is set to be about 0.1Hz, corresponding to a setting time of about 6sec. Figure

<sup>3</sup>Because the reference PZT is mounted with opposite polarization, a phase shift of  $180^\circ$  is introduced in the frequency response of  $V_L/V_{ref}$ .

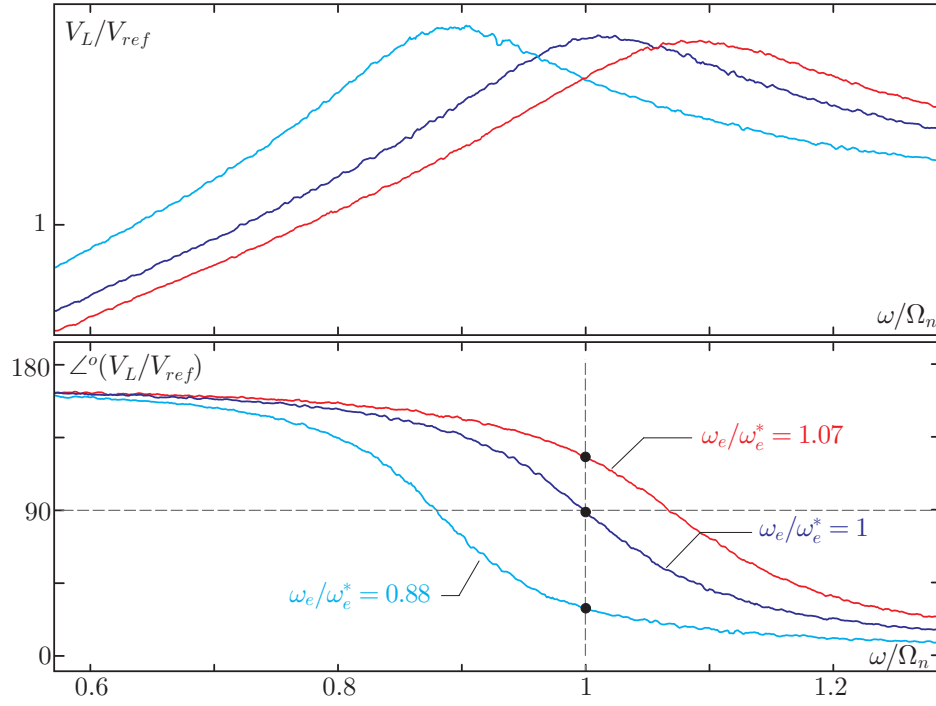


Figure 13. Measured magnitude and phase of  $V_L/V_{ref}$  for various values of  $\omega_e$ .

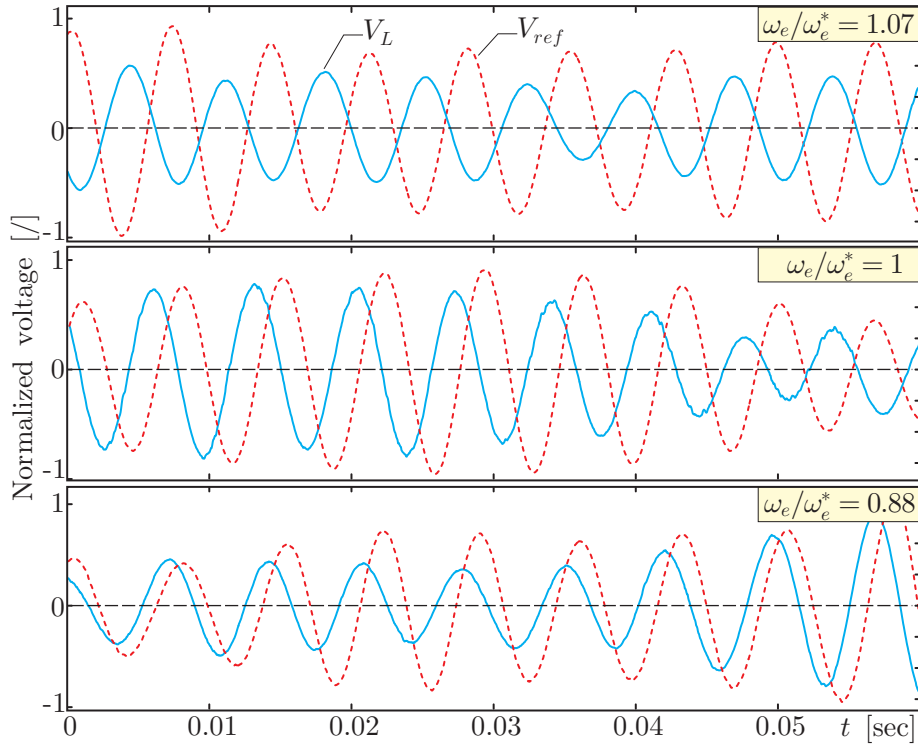


Figure 14. Time response of  $V_L$  and  $V_{ref}$  for various values of  $\omega_e$ .



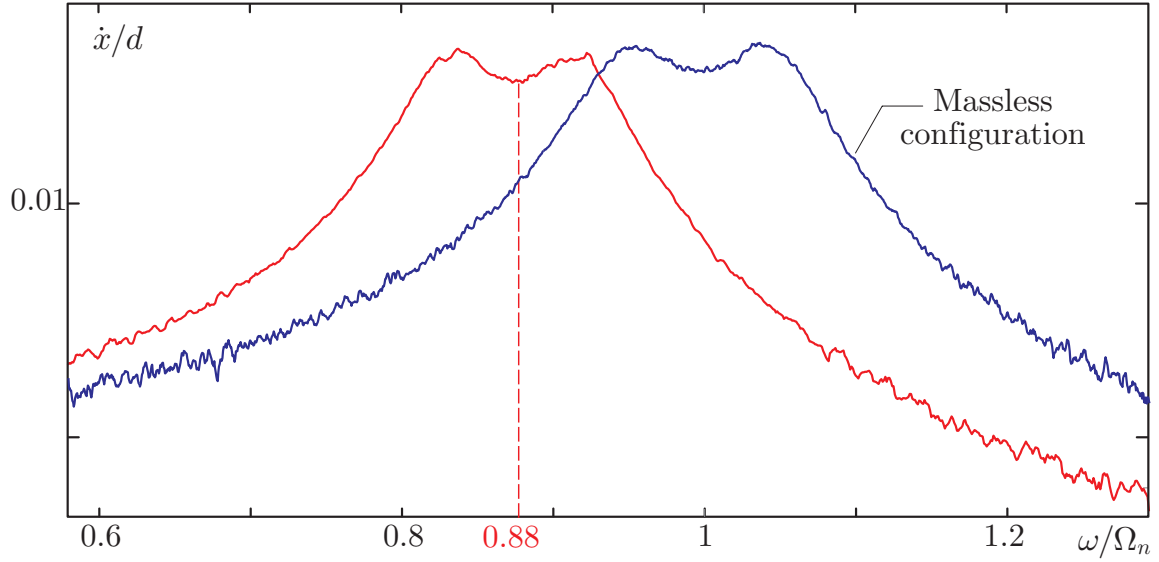


Figure 15. Frequency response function of the beam tip without shunt, with optimally tuned RL shunt, and with mistuned RL shunt.

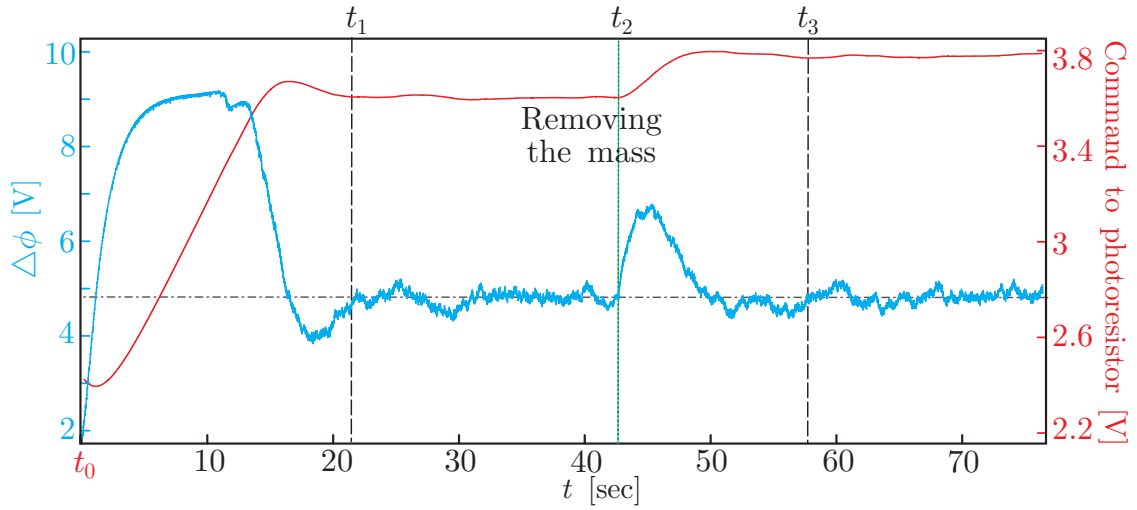


Figure 16. Due to imperfection of the electrical components, the voltage which corresponds to  $\pi/2$  of relative phase shift is not 5Volts, but 4.8Volts

16 shows the measured relative phase  $\Delta\phi$  in volts, and the evolution of the command of the voltage controlled synthetic inductor. First, the cantilever beam is equipped with the optional mass and the RL shunt is tuned such that  $\omega_e \ll \Omega_n$ ; at  $t_0$ , the Phase Shift to Voltage Converter circuit is plugged and the control is turned on. Few seconds are needed by the circuit to measure the relative phase shift, and as long as  $\Delta\phi < \pi/2$  (or 4.8Volts), the voltage commanding the synthetic inductor increases until  $t_1$  where  $\Delta\phi \leq -\pi/2$  (corresponding to  $\omega_e = \Omega_n$ ). At  $t_2$ , the optional mass is removed from the beam and  $\Delta\phi$  becomes larger than  $\pi/2$ , leading to a reaction of the controller to compensate this change, and at  $t_3$  the control system converges to the optimal value of  $L$ . The fluctuation of the measured  $\Delta\phi$  is due to the fact that the instantaneous frequency is not exactly  $\Omega_n$ . however, the average value of  $\Delta\phi$  corresponds to the relative phase at the average frequency  $\Omega_n$ .

## 6. CONCLUSION

This paper investigates the linear RL shunt damping when a single mode is targeted. The importance of the relative phase shift between the strain at the location of the transducer and the electrical charge of the RL circuit is highlighted and supported experimentally. At resonance, the relative phase shift between the strain at the location of the piezoelectric transducer and the electric charge in the transducer must be in quadrature of phase in order to preserve the optimal performance of the RL shunt.

The problem related to the robustness of the RL shunt with respect to the variability of the resonance frequency has been solved by adapting the value of the inductor  $L$ , via a voltage controlled synthetic inductor. A Phase Shift to Voltage Converter, inspired from a phase locked loop circuit, offers the possibility to measure accurately the relative phase shift between two reference signals, and the output is used to adapt the value of the inductor.

## ACKNOWLEDGEMENT

This research is supported by the Wallonia Region of Belgium through the Mecatech M4 Project.

## References

- [1] Niederberger D. *Smart Damping Materials Using Shunt Control*. PhD thesis, Swiss Federal Institute of Technology - ETHZ, 2005.
- [2] Niederberger, D., Morari, M., and Pietrzko, S. J. *Adaptive resonant shunted piezoelectric devices for vibration suppression*. In Smart Structures and Materials (pp. 213-224), International Society for Optics and Photonics, 2003.
- [3] Niederberger, D., Fleming, A., Moheimani, S. R., and Morari, M. *Adaptive multi-mode resonant piezoelectric shunt damping*. Smart Materials and Structures, 13(5), 1025, 2004.

- [4] PHILBRICK RESEARCHES, Inc. *Application Manual for Computing Amplifiers for Modeling, Measuring, Manipulating and Much Else*. Nimord Press, Boston, 1965.
- [5] Forward R. L. *Electronic Damping of Vibration in Optical Structures*. Journal of Applied Optics, 18(5): 690-697, 1979a.
- [6] Forward R. L. *Electromechanical Transducer-Coupled Mechanical Structure with Negative Capacitance Compensation Circuit*. US Patent 4,158,787, 1979b .
- [7] Hagood N.W. and von Flotow A. *Damping of Structural Vibrations with Piezoelectric Materials and Passive Electrical Networks*. Journal of Sound and Vibration, 146(2): 243-268, 1991.
- [8] Hollkamp J.J. *Multimodal Passive Vibration Suppression with Piezoelectric Materials and Resonant Shunts*. Journal of Intelligent Material Systems and Structures, 5(1):49-57, 1994.
- [9] Hollkamp, J. J., and Starchville, T. F. *A self-tuning piezoelectric vibration absorber*. Journal of Intelligent Material Systems and Structures, 5(4), 559-566, 1994.
- [10] Richard C., Guyomar D., Audigier D. and Bassaler H. *Enhanced Semi Passive Damping Using Continuous Switching of a Piezoelectric Device on an Inductor*. Proceeding of the SPIE international Symposium on Smart Structures and Materials. Conference, Passive Damping and Isolation, Newport Beach, 3989:288-299, 2000.
- [11] Preumont A. *Mechatronics, Dynamics of Electromechanical and Piezoelectric Systems*. Springer, 2006.
- [12] Lefeuvre E., Badel A., Petit L., Richard C. and Guyomar D. *Semi-Passive Piezoelectric Structural Damping by Synchronized Switching on Voltage Sources*. Journal of Intelligent Matrial, Systems and Structures. 17(8-9):653-60, 2006.
- [13] De Marneffe, B., and Preumont, A. *Vibration damping with negative capacitance shunts: theory and experiment*. Smart Materials and Structures, 17(3), 035015, 2008.
- [14] Mokrani, B., Rodrigues, G., Burda, I., Bastaits, R., and Preumont, A. *Synchronized switch damping on inductor and negative capacitance*. Journal of intelligent material systems and structures, 2012.
- [15] E. Carrera, S. Brischetto, P. Nali, *Plates and Shells for Smart Structures: Classical and Advanced Theories for Modeling and Analysis*. John Wiley & Sons, Chichester, 2011.
- [16] A. Benjeddou, M. Hamdi, S. Ghanmi, *Robust inverse identification of piezoelectric and dielectric effective behaviors of a bonded patch to a composite plate*. *Smart Structures and Systems*, **12**, 523-545, 2013.